Composites Science and Technology 226 (2022) 109541

Contents lists available at ScienceDirect

Composites Science and Technology

journal homepage: www.elsevier.com/locate/compscitech

Polyimide/boron nitride composite aerogel fiber-based phase-changeable textile for intelligent personal thermoregulation

Qiaoran Zhang [a], Tiantian Xue [a], Jing Tian [a], Yi Yang [a], Wei Fan [a,*], Tianxi Liu [a,b,**]

[a] State Key Laboratory for Modification of Chemical Fibers and Polymer Materials, College of Materials Science and Engineering, Donghua University, Shanghai, 201620, China

[b] Key Laboratory of Synthetic and Biological Colloids, Ministry of Education, School of Chemical and Material Engineering, Jiangnan University, Wuxi, 214122, China

ARTICLE INFO

Keywords:
Polyimide
Boron nitride
Phase-changeable materials
Aerogel fiber
Intelligent thermoregulation

ABSTRACT

Aerogel fibers, which are beneficial for enhancing the thermal response and preventing the leakage of phase-changeable materials (PCMs) during phase change process, are excellent candidates for phase-changeable textiles with excellent thermoregulating performance. Herein, polyimide/boron nitride (PI-BN) composite aerogel fibers with highly porous structure and good mechanical strength have been prepared by freeze-spinning technique, which could be served as the heat conduction path and skeleton for PCMs. Into the pores of the PI-BN aerogel textile was incorporated polyethylene glycol (PEG) by vacuum impregnation to obtain phase-changeable PI-BN/PEG textile. The high thermal conductivity of PI-BN skeleton could endow the quick thermal response rate of PI-BN/PEG textile upon the phase change process, while the high porosity of aerogel fiber could allow high loading of PEG and inhibit liquid leakage during phase change process. The resultant PI-BN/PEG composite textile has high thermal conductivity (5.34 W m^{-1} K^{-1}), high enthalpy (125.2 J g^{-1}) and excellent work stability after 100 heating-cooling cycles, accounting for the desired thermoregulating performance. Moreover, polydimethylsiloxane (PDMS) has been coated on the surface of PI-BN/PEG textile, endowing the textile hydrophobicity, waterproofness and washability, indicating its great potential as candidate for personal thermal management.

1. Introduction

Recently, thermo-regulating textiles that can be able to provide personal thermal management have attracted significant attention [1–5]. Previous studies reveal that stimuli-responsive materials especially phase change materials (PCMs) with good responses to varying temperature, can be used to fabricate responsive intelligent textiles so as to well adjust human body temperature [6,7]. Possessing a high enthalpy of fusion, PCMs can absorb or release heat temporarily, thereby producing a temporary cooling or heating effect during the phase change process and maintaining the microclimate in a constant temperature. Application of PCMs in textiles provides a thermal barrier effect against the environmental temperature fluctuations, which make them exceptional candidates for fabricating intelligent thermoregulating textiles.

Due to the inherent liquid leakage issue of PCMs in the process of phase change, PCMs such as paraffin, stearic acid, and polyethylene glycol (PEG) are usually incorporated into traditional textiles in the form of microcapsules by coating [8] or electrospinning [9]. For instance, Sánchez et al. [10] has developed the thermo-regulating textiles using paraffin wax microcapsules, and the as-prepared coating fabric with 35 wt% of microcapsules showed a heat latent storage of 7.6 J g^{-1}. Lu et al. [11] has prepared a phase-changeable textile with core-sheath structure fabricated by coaxial electrospinning, which possesses an enthalpy of 60.3 J g^{-1} with the encapsulation efficiency of 54.3%. Yu et al. [12] has prepared corncoblike nanofibers by incorporating n-octadecane phase change capsules, which has favorable thermoregulating performance with phase change heat latent of 75 J g^{-1}. Although traditional strategies abovementioned to obtain PCM-based intelligent textiles were relatively sophisticated, they still exist the shortcomings of low phase change enthalpy due to limited loading of PCM, resulting in the poor thermal management capability that limits their practical applications.

* Corresponding author.

** Corresponding author. State Key Laboratory for Modification of Chemical Fibers and Polymer Materials, College of Materials Science and Engineering, Donghua University, Shanghai 201620, China.

E-mail addresses: weifan@dhu.edu.cn (W. Fan), txliu@dhu.edu.cn, txliu@fudan.edu.cn (T. Liu).

https://doi.org/10.1016/j.compscitech.2022.109541
Received 28 March 2022; Received in revised form 13 May 2022; Accepted 19 May 2022
Available online 25 May 2022

Aerogel fibers, combining the high porosity of aerogels with the large length-to-diameter ratio of fibers, exhibit fascinating performances such as good flexibility and lightweight [13]. More importantly, similar to bulk aerogels, the three-dimensional interconnected porous network of aerogel fibers with high porosity as well as large capillary force could allow to encapsulate a large amount of PCMs [14–16]. On the one hand, the high loading of PCMs in the aerogel fiber can help to increase the latent heat of the composite phase change fiber, which is favorable for enhancing the energy storage/release ability. On the other hand, the aerogel fiber as a skeleton can prevent the leakage of PCMs during phase change process due to its capillary force. In the past years, more and more efforts have been dedicated to develop phase-changeable aerogel fibers by using graphene aerogel fiber [17], silica aerogel fiber [18], Kevlar aerogel fiber [19], and MXene aerogel fiber [20]. For instance, Li et al. [17] has fabricated a graphene-aerogel-directed phase-change smart fibers by impregnating organic PCM into graphene aerogel fibers, which has tunable functions of thermal conversion and storage response to external stimuli. Lyu et al. [19] has obtained phase-changeable fibers by submerging nanofibrous Kevlar aerogel fibers in the melting PEG1000, which has high energy storage property with phase change enthalpy of 162 J g^{-1}. However, poor mechanical strength (tensile strength normally below 2.6 MPa) of current aerogel fibers may limit their practical applications for wearable textiles. Fortunately, polyimide (PI) aerogel fibers with outstanding mechanical property and excellent thermal stability have been prepared via different technologies such as freeze spinning-freeze drying [21], wet spinning-freeze drying [13], and sol-gel closed transition-supercritical CO_2 drying [22]. Hence, PI aerogel fiber may be a good candidate as a skeleton for encapsulation of PCMs with high loading, obtaining PI-aerogel-based phase-changeable fiber. However, due to the inherent low thermal conductivity of organic materials, PI aerogel/PCM composite fiber may still face the key issue of slow thermal response rate during the phase change process [23–28]. Thermal conductive nanoparticles, especially boron nitride (BN) nanosheets with advantages of excellent thermal conductivity and chemical resistance, have been widely utilized for enhancing the thermal conductivity of polymers [29,30]. Hence, it is still a challenge to significantly increase the thermal conductivity of aerogel/PCM composite fibers without sacrificing their mechanical performance.

Herein, an intelligent thermo-regulating textile has been reported by impregnating PCMs into polyimide-boron nitride nanosheet (PI-BN) composite aerogel fiber. Specifically, PI-BN aerogel fiber has been prepared by freeze-spinning, resulting in a highly porous structure and excellent mechanical strength, which was suitable for preparing high-performance phase-changeable textile. Firstly, PI-BN aerogel fiber has a high thermal conductivity, due to incorporation of BN nanosheets, leading to quick thermal response upon external temperature change. Secondly, high porosity of the PI-BN composite fiber could realize high loading of PCMs, obtaining the phase-changeable textile with high enthalpy. Last but not least, the skeleton of PI-BN aerogel fiber could well confine the melting PCMs and prevent their leakage due to its capillary force. The resultant phase-changeable PI-BN/PEG composite textile exhibits good mechanical strength, high phase change enthalpy and excellent work stability after 100 heating-cooling cycles, superior to other PCM-based textiles reported previously. Furthermore, polydimethylsiloxane (PDMS) has been coated on the textile surface, endowing the textile hydrophobicity, waterproofness and washability. Therefore, the as-prepared PI-BN/PEG textile with excellent mechanical and thermal-regulating property, exhibits great potential as exceptional candidates for intelligent personal thermoregulation.

2. Experiment

2.1. Materials

Hexagonal boron nitride (h-BN) with a horizontal size of 1–2 μm was purchased from Aladdin Reagent. 3,3′,4,4′-biphenyl tetracarboxylic dianhydride (BPDA), 4,4′-oxydianiline (ODA), N, N-dimethylacetamide (DMAc), triethylamine (TEA), and PEG-1000 were commercially obtained from Sinopharm Chemical Reagent Company Limited. Polydimethylsiloxane (PDMS) precursor and its curing agent were supplied by Dow Corning.

2.2. Fabrication of PI-BN aerogel fiber

BN nanosheets were obtained via the process of thermal oxidation, and exfoliation method reported previously [31]. Water-swellable polyamic acid (PAA) were synthesized by ODA and BPDA with the help of TEA according to our previous work [32,33]. The PAA-BN solutions containing different concentration of BN nanosheets were used as the spinning solution. Briefly, 1 g of PAA solid was dissolved in the aqueous dispersion of BN nanosheets (3, 6, 9 and 12 mg mL^{-1}, respectively), and then 0.5 g TEA as a cosolvent was added with stirring for 1 h, to obtain stable PAA-BN solution. Subsequently, the obtained PAA-BN solution was stand for another 1 h for gelation and extruded with a pump-controlled syringe to afford PAA-BN fiber via freeze-spinning process. The as-prepared PAA-BN fibers were then freeze-dried and sequentially heated in a tube furnace under N_2 atmosphere to complete thermal imidization, thereby yielding PI-BN aerogel fibers. PI-BN aerogel fibers with different content of BN were denoted as PI-BN_3, PI-BN_6, PI-BN_9 and PI-BN_{12}, respectively.

2.3. Fabrication of phase-changeable PI-BN/PEG textile

PI-BN aerogel fibers were knitted to obtain PI-BN aerogel textile. PEG-1000 was heated at 80 °C in a vacuum oven to achieve complete melting. The as-knitted PI-BN aerogel textile was immersed in the molten PEG and kept overnight at 80 °C under vacuum to achieve saturated adsorption of PEG. Excess PEG attached to its surface was removed by the filtered paper, followed by cooling to room temperature, obtaining phase changeable PI-BN/PEG textile. Similarly, PI/PEG textile was also prepared. For endowing the textile waterproofness, PDMS was coated on PI-BN/PEG textile (denoted as M-PI-BN/PEG). Specifically, the PI-BN/PEG textile was immersed in 60 mL of anhydrous ethanol containing 2 g of PDMS precursor with its curing agent (0.2 g), and maintained at 60 °C for 1 h.

2.4. Characterization

X-ray powder diffraction (XRD) patterns were obtained with an X-ray Diffractometer (D2 PHASER, Germany). Fourier transform infrared spectra (FTIR) were recorded with a Nicolet6700 FT-IR spectrophotometer (Bruker Spectrum Instruments, USA). The morphology as well as the corresponding EDS mapping image were observed by field-emission scanning electron microscopy (FESEM-7500F, Japan). Mechanical tests were conducted in the tensile mode with an electronic universal testing instrument (SANS UTM2102, China). The thermal conductivity was tested with a TPS 2500S hot disk thermal constant analyzer (Swedish Hot Disk Ltd, Sweden). The thermogravimetric curves under nitrogen atmosphere were measured with a thermogravimetric analyzer (TG, Netzsch TG 209 F1 Libra, Germany). A Q20 Differential scanning calorimetry (DSC, TA, USA) was conducted to evaluate the thermal properties of PEG, PI/PEG and PI-BN/PEG samples in the temperature range of −10–110 °C at a constant heat rate of 10 °C min^{-1}. The relative enthalpy values were calculated via integrating subplot regions in DSC plots. Infrared thermal imaging camera (FOTRIC 226s, China) was used to detect the temperature distribution of textiles on the hot stage, and the working distance was around 30 cm. The surface temperatures of textiles were recorded by thermal couples (175T2, testo Co., Ltd, China). The water contact angles were tested with a DSA-100S optical contact-angle system (OSA200, Germany) at room temperature. The porosity of PI aerogel fiber was calculated using the following equation:

$$P = \left(1 - \frac{\rho_0}{\rho}\right) \times 100\%$$

where P is the porosity, ρ_0 is the apparent density, and ρ is the skeletal density, which is estimated from the weighted density of polyimide and BN (1.57 g/cm^3).

3. Results and discussion

Fig. 1a shows the schematic diagram for the preparation of PI-BN/PEG composite textile, where the main steps include freeze-spinning, imidization, and infusion. Briefly, a well-dispersed PAA-BN spinning solution (digital photo shown in Fig. S1) was extruded from a syringe, and then slowly passed through a cold copper ring, to freeze the fiber gradually. After subsequent freeze-drying and thermal imidization, PI-BN fiber could be obtained with a highly porous structure. A roll of PI-BN aerogel fiber with light yellow color is shown in Fig. 1b, indicating the good spinnability and scalability. Moreover, a single PI-BN aerogel fiber can withstand a weight of 200 g, indicating its good mechanical strength (Fig. 1c). The porosity of PI-BN aerogel fibers is around 88% (Table S1), which is conducive to endow the high loading of PEG within the porous structure. With the highly porous structure and good mechanical strength, the PI-BN aerogel fiber can be woven into textile and allow to encapsulate PEG, resulting in phase-changeable PI-BN/PEG composite textile (Fig. 1d). The PI-BN/PEG composite textile can be bended and folded (Fig. 1e), demonstrating its good flexibility, providing the possibility as wearable clothing.

The radial cross-sectional SEM images of PI and PI-BN aerogel fibers are given in Fig. 2a and b. Both PI and PI-BN aerogel fibers exhibit similar three-dimensional porous structure induced by freeze-drying, of which the pore size mainly distribute in the range of 10–100 μm. And BN nanosheets is distributed homogeneously among the PI-BN aerogel fiber, as evidenced by relevant TEM image (inset in Fig. 2b) and EDS element mappings (Fig. 2c). The mechanical properties of PI and PI-BN aerogel fibers were characterized by stress-strain curves shown in Fig. S2. As shown in Fig. S2, PI-BN aerogel fibers exhibit higher tensile strength than pure PI aerogel fiber. In particular, the PI-BN$_6$ aerogel fiber has an optimized tensile strength of up to 26 ± 0.7 MPa. Besides, the thermal conductive performance of PI-BN aerogel fibers with different content of BN nanosheets was evaluated by infrared pictures as shown in Fig. S3a. The as-prepared aerogel fibers were placed on a hot stage (150 °C) and the temperature difference (|ΔT|) between the fiber surface and the hot stage was summarized in Fig. S3b. Compared with pure PI aerogel fibers, the PI-BN$_6$ aerogel fibers show a largely decreased |ΔT|, indicating the significantly improved thermal conductivity due to the incorporation of BN nanosheets. However, further increasing the content of BN nanosheets in the aerogel fiber only shows a slight decrease of |ΔT|. Therefore, combined with the corresponding mechanical strength, PI-BN$_6$ aerogel fiber is selected to fabricate PI-BN aerogel textile for further research.

After the incorporation of PEG, PEG was fully infused in the PI-BN aerogel fibers, in association with the disappearance of the porous structure upon the PEG incorporation (Fig. 2d). For determining the components of the as-prepared fibers, the corresponding FTIR spectra are shown in Fig. 2e. As for the FT-IR spectra, PI aerogel fiber has the typical characteristic absorption peaks at 1711 cm^{-1} and 1773 cm^{-1}, which are respectively attributed to the symmetrical and asymmetrical stretching of the C=O group. Besides, the absorbance band at 1367 cm^{-1} is corresponded to the C–N stretching vibration of imide rings [13]. Different from pure PI fiber, B–N–B out of plane bending vibration at 805 cm^{-1} assigned to the BN nanosheets is appeared for the spectra of PI-BN aerogel fiber, indicating the successful incorporation of BN nanosheets [31]. As for PI-BN/PEG composite fiber, the appearance of C–H vibration peaks at 2923 cm^{-1} prove the incorporation of PEG in PI-BN aerogel fiber [34], reflecting the successful preparation of PI-BN/PEG composite fiber. The thermal stability of PI-BN/PEG aerogel fibers and the content of PEG within the phase-changeable composite fiber were evaluated by TGA (Fig. 2f) and corresponding data were summarized in Table S2. As depicted in Fig. 2f, PI aerogel fiber exhibits excellent thermal stability and undergoes thermal decomposition around 500–600 °C with 33.6 wt% char residue at evaluation temperature [35]. Compared with the pristine one, PI-BN composite aerogel fiber has the similar decomposition trend, which has higher residue of 53.8 wt% at 800 °C, due to the incorporation of BN nanosheets. Different from PI and PI-BN aerogel fiber, the phase-changeable PI-BN/PEG

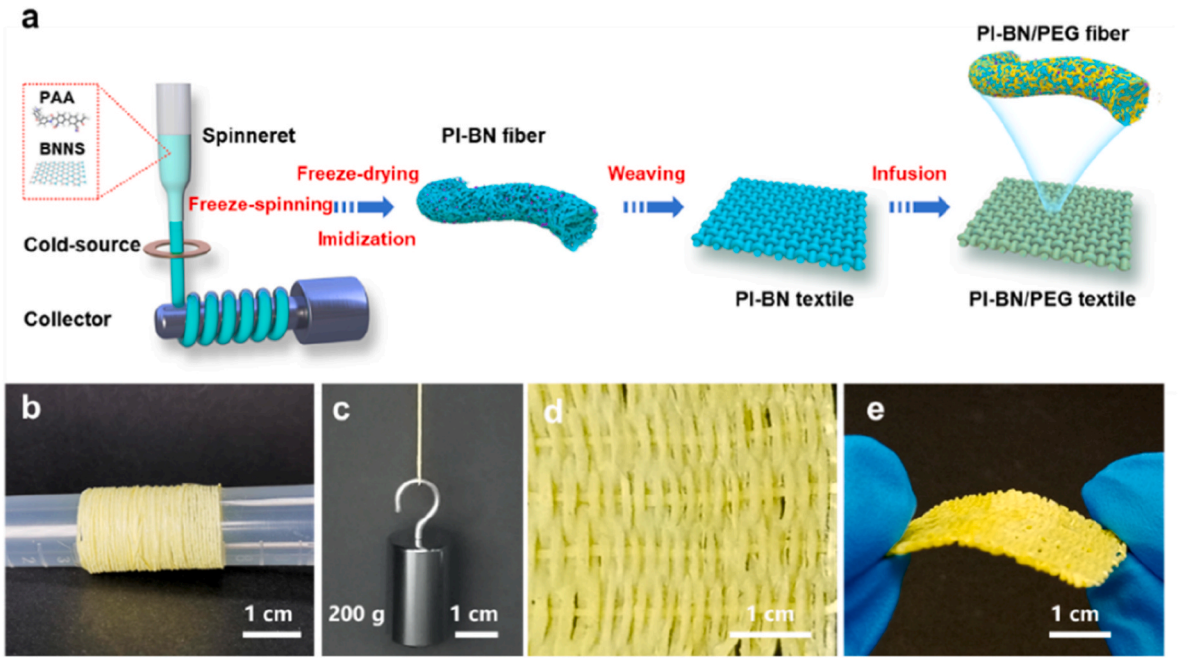

Fig. 1. Fabrication of phase-changeable PI-BN/PEG composite textile. (a) Schematic illustration of the preparation of PI-BN/PEG textile. (b) Digital photos of PI-BN aerogel fiber. (c) Optical image showing a PI-BN aerogel fiber hanging 200 g weight, indicating its high strength. (d, e) Optical image of the as-prepared PI-BN/PEG textile.

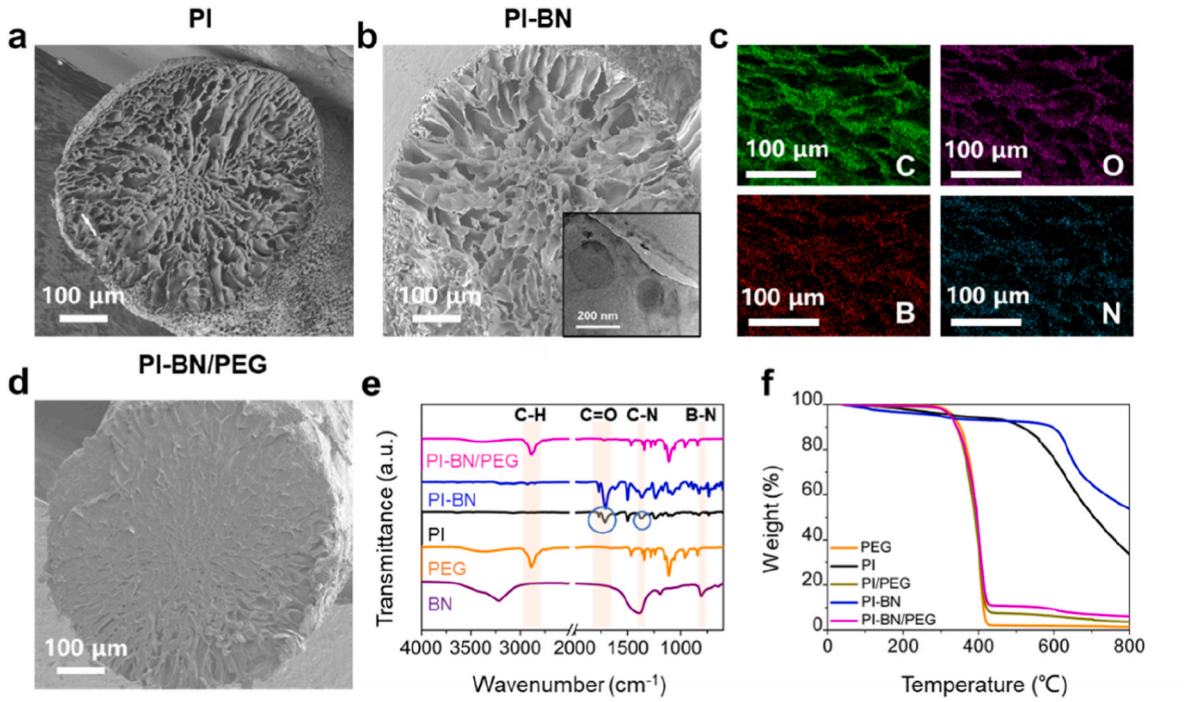

Fig. 2. Microstructure and properties of PI-BN/PEG composite fibers. (a) Radial cross-sectional SEM images of PI aerogel fiber. (b) Radial cross-sectional SEM image as well as TEM image (inset) of PI-BN aerogel fiber, and (c) corresponding EDS images. (d) Radial cross-sectional SEM image of PI-BN/PEG fiber. (e) FTIR spectra and (f) TG curves of the as-prepared PI-based composite fibers.

composite fiber undergoes thermal decomposition around 350 °C, due to the decomposition of PEG. According to the residue of the TGA curves, the loading (mass fraction) of PEG in the PI-BN/PEG composite fiber is as high as 89.0%, which is beneficial for high phase-change enthalpy.

High thermal conductivity and high phase change enthlpy are two key factors for phase-changeable textiles. As dipicted in Fig. 3a, with the incorporation of BN nanosheets, PI-BN/PEG textile has much enhanced thermal conductivity (5.34 W m^{-1} K^{-1}) as compared with that of PI/PEG (0.44 W m^{-1} K^{-1}), contributing to the quick response rate in the process of phase change and higher latent heat retention of PCM. The melting

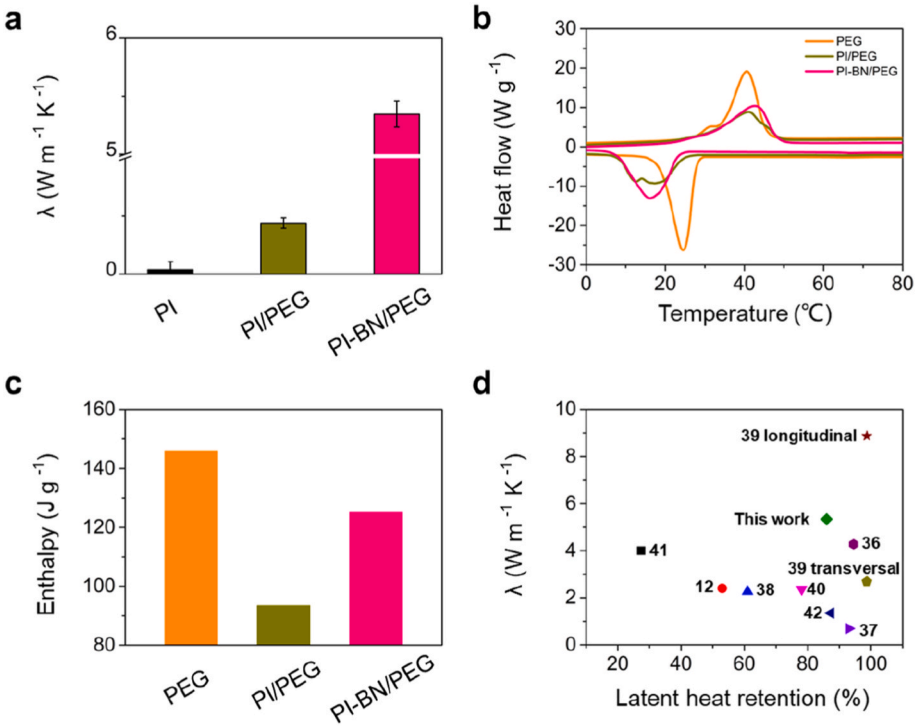

Fig. 3. Thermal conductivity and phase change enthalpy of PI-BN/PEG textile. (a) Thermal conductivity of PI, PI/PEG and PI-BN/PEG textile at room temperature. (b) DSC curves and (c) corresponding enthalpy of PEG, PI/PEG and PI-BN/PEG textile. (d) Comparison of latent heat retention as well as thermal conductivity of PI-BN/PEG textile with other PCM-based composites reported previously.

point and phase change enthalpy of PI-BN/PEG textile measured by DSC are provided in Fig. 3b and c, and the corresponding data are summarized in Table S3. The as-prepared PI-BN/PEG textile has a melting temperature (T_m) of about 29.0 °C (Fig. 3b), close to human body temperature, which could be potentially applied as personal thermoregulating textile with phase-changeable performance. In addition, the PI-BN/PEG texitle has a high phase change enthalpy of 125.2 J g^{-1}, just a little smaller than that of PEG (145.8 J g^{-1}) and much higher than that of PI/PEG (93.5 J g^{-1}), which is ascribed to the high loading of PCM (89.0%) and high thermal conductivity of the PI-BN skeleton. As shown in Table S4, the enthalpy of PI-BN/PEG textile is superior to that of other phase changeable textiles previously reported [36]. More importantly, the latent heat retention of our textile is as high as 86% with high thermal conductivity of 5.34 W m^{-1} K^{-1}, which were much superior to those of PCM-based reported previously shown in Fig. 3d [37–43]. Therefore, the PI-BN/PEG texitle with large phase change enthalpy contributes to high energy storage capacity, which, in combination with the relatively appropriate melting temperature, is expected to be a smart textile for personal thermal management.

The working stability of phase-changeable textiles is critical to their practical applications. The thermal stability of PI-BN/PEG textile after 20, 40, 60, 80, and 100 heating-cooling cycles was evaluated by DSC tests. As shown in Fig. 4a and b, the melting/freezing temperature of PI-BN/PEG textile stays at 29.0 °C/23.3 °C and varys slightly after 100 heating-cooling cycles. Besides, the PI-BN/PEG textile possesses high melting phase change enthalpy of 124.9 J g^{-1} after continuous 100 cycles without obvious change, which demonstrates its good thermal stability during alternate heating-cooling cycles (Fig. 4c and d). The SEM images of the PI-BN/PEG fiber before and after 100 heating-cooling cycles are presented in Fig. 4e. The PI-BN/PEG fiber retains almost the original morphology after 100 heating-cooling cycles, illustrating its good structural stability, which can be attributed to the strong capillary force of the aerogel fibers that firmly fixes PEG within the porous structure. As shown in Fig. 4f, PEG is melted into liquid in association with the damage of its shape when heated above the melting point of PEG (80 °C). In contrast, no obvious leakage of PEG is observed for the PI-BN/PEG textile under the same condition, indicating that PEG is firmly encapsulated in the PI-BN/PEG textile, which features excellent stability and repeatability for thermoregulation.

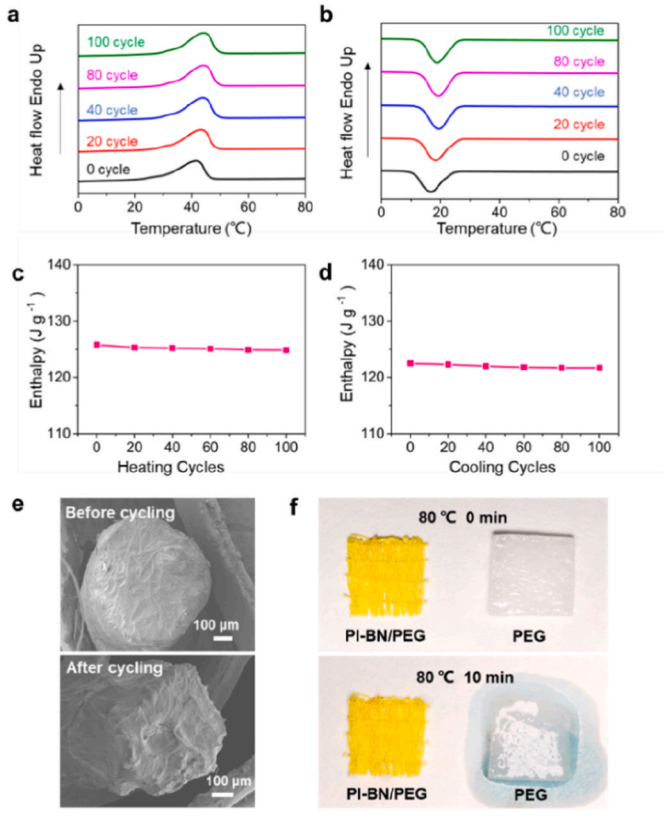

Fig. 4. The cycling stability of phase-changeable PI-BN/PEG textile. DSC curves of PI-BN/PEG textile after different (a) heating and (b) cooling cycles. Enthalpy of PI-BN/PEG textile after different (c) heating and (d) cooling cycles. (e) Cross-sectional SEM images of PI-BN/PEG textile before and after 100 heating/cooling cycles. (f) Optical image of PI-BN/PEG and PEG at 80 °C for 0 min and 10 min.

As a proof of concept for evaluating the thermoregulation property of PI-BN/PEG textile in practical conditions, the surface temperature of textile were recorded by the infrared thermal camera as well as thermocouple by placing it on a temperature-adjustable stage, simulating the variable temperature environment. The stage was first heated from 25 °C to 80 °C and then cooled to 25 °C. Fig. 5a gives the corresponding infrared thermal images of commercial cotton, PI/PEG and PI-BN/PEG textiles at different moments on the hot stage during the heating and cooling. As shown in Fig. 5a, different from comercial cotton, PI/PEG and PI-BN/PEG textile both have obvious delay in temperature change during heating and cooling process, which corresponds to the latent heat storage upon the liquification and heat release upon the solification of PEG. Especially, PI-BN/PEG textile has higher temperature than that of PI/PEG at time of t_1 (beginning of melting phase change process), which is due to the high thermal conductivity of PI-BN aerogel fiber by incorporating BN nanosheets, leading to the quick response rate during the process of phase change. Besides, the surface of PI/PEG and PI-BN/PEG textile are just 38.0 °C and 41.6 °C at the time of t_2 (ending of melting phase change process), much lower than that of commercial cotton (58.3 °C), reflecting the excellent cooling effect in the hot environment. During the cooling process, PI-BN/PEG also exhibits much higher surface temperature than that of commercial cotton and PI/PEG at the time of t_4 and t_5, with 9 °C higher than that of commercial cotton, indicating its outstanding warming property with quick response rate in cold environment. The corresponding variations of surface temperature of the textiles on the hot stage were further recorded by thermocouple and the temperature-time curves are shown in Fig. 5b. As shown in Fig. 5b, different from that of commercial cotton, the curves of phase-changeable PI/PEG and PI-BN/PEG textiles both present a obvious platform around 32.0–37.0 °C during the process of heating and cooling, corresponding to the phase change temperature of PEG, well consistenting with relevant DSC curves. It is worth noting that the slope of the temperature-time curve of PI-BN/PEG is larger than that of PI/PEG at the beginning of heating process, which is due to the high thermal conductivity of PI-BN that could accelerate the thermal response of the fibers. The enhanced thermal response rate could promote the occurrence of the phase change process, thereby realizing rapid and intelligent temperature adjustment. Besides, PI-BN/PEG has longer temperature platform (~350 s) during both heating and cooling than that of PI/PEG (~220 s), corresponding to its higher phase change enthlpy, which could postpone the temperature change upon the change of environment temperature. Additionally, when the heating-cooling process is repeated, the phase-changeable textile still exhibits stable surface temperature as that of before, corresponding to excellent reliability for thermoregulation of the PI-BN/PEG textile. Moreover, the stability of PI-BN/PEG textile is further tested during the 10 heating-cooling cycles (Fig. S4), and the equilibrium surface temperature of PI-BN/PEG textile is recorded in Fig. 5c. When the hot stage temperature is adjusted within the range of 25.0–80.0 °C, the textile surface temperature is within the range of 25.5–70.6 °C, which indicates that the PI-BN/PEG textile exhibits outstanding cycling stability for long-term thermoregulation.

The thermoregulating mechanism of the phase-changeable PI-BN/PEG textile is illustrated in Fig. 5d. Briefly, the phase-changeable PI-BN/PEG textile can be quickly liquified under a hot environment, thereby storaging heat energy during the melting phase change process and

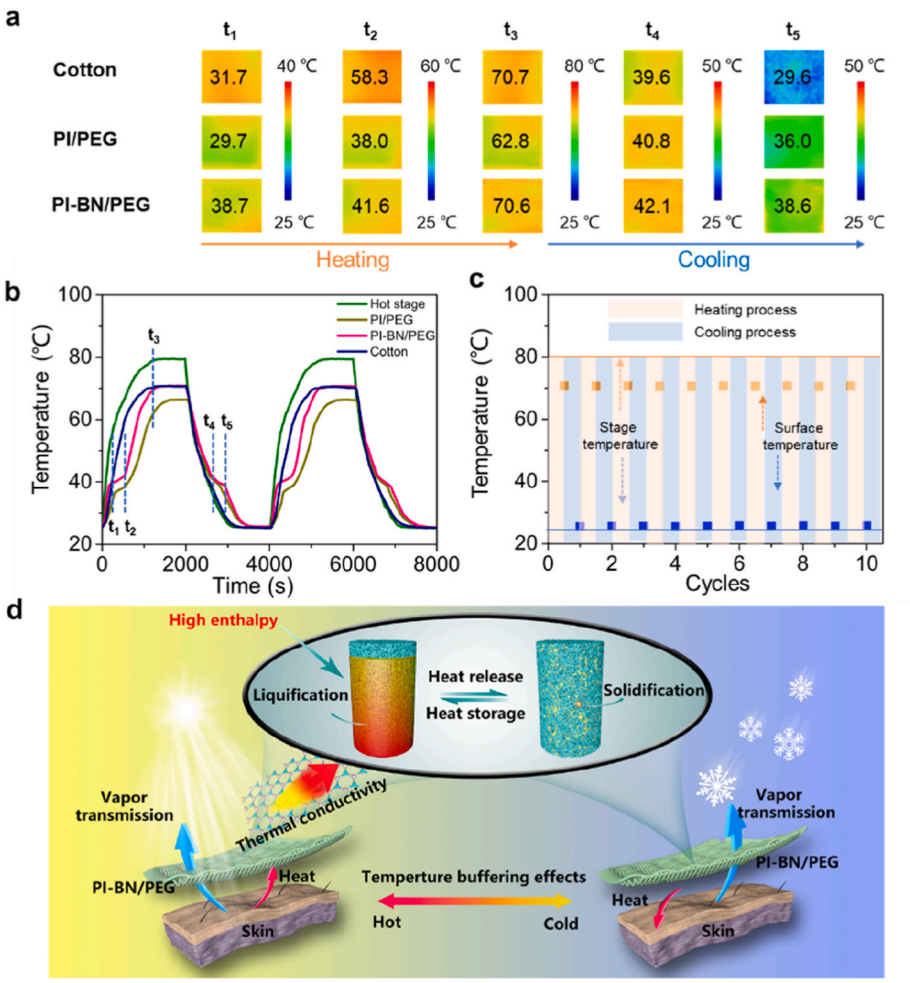

Fig. 5. Thermal regulating properties of PI-BN/PEG textile. (a) Infrared thermal images of cotton, PI/PEG and PI-BN/PEG textiles during heating and cooling process. (b) The temperature-time curves of cotton, PI/PEG and PI-BN/PEG textiles recorded by thermocouple. (c) The cycling stability of PI-BN/PEG textile on the hot stage with the temperature range from 25 to 80 °C. (d) Schematic illustration of the thermoregulating performance of PI-BN/PEG textile.

preventing noticeable increase of temperature. Under very cold environment, vice versa, the phase-changeable PI-BN/PEG textile would be solidified to release heat, thereby preventing significant decrease of temperature. The superior thermoregulating performance is mainly based on the following several factors. Firstly, the high thermal conductivity of PI-BN skeleton could endow the quick thermal response rate of PI-BN/PEG textile upon the occurrence of phase change process, presenting superior temperature sensitivity as well as quick heat transfer rate for the phase change process. Furthermore, this high thermal conductivity of PI-BN will significantly improve the latent heat retention of PCM, leading to a large phase change enthalpy. Secondly, the large phase change enthalpy enables PI-BN/PEG textile to postpone the temperature change in the hot or cold environment for efficient thermoregulating performance. Moreover, the appropriate melting point of PI-BN/PEG textile that close to the comfortable body temperature, makes them have great potential for achieving the thermal comfort of the wearer.

The waterproof behavior as well as moisture permeation of PI-BN/PEG textile are also key factors in terms of its practical thermoregulating applications. For protecting the hydrophilic PI-BN/PEG aerogel textile against moisture or water penetration, a hydrophobic protection layer of PDMS was coated on the surface of PI-BN/PEG textile (M-PI-BN/PEG), and the corresponding FTIR spectra evidenced the successful coating (Fig. S5). Fig. S6 compares the moisture permeation of PI-BN/PEG, M-PI-BN/PEG and commercial cotton. Although the moisture permeation of M-PI-BN/PEG textile is slightly lower than that of PI-BN/PEG, it still shows a similar performance as commercial cotton, suppling good breathability for wearers. As shown in Fig. S7a, the water contact angle of PDMS coated PI-BN/PEG textile is around 92.7°, corresponding to hydrophobic property. The hydrophobic property endows the textile excellent waterproof performance, which shows resistance to various liquids, such as milk, tea and coffee (Fig. S7b). Moreover, for evaluating the washing durability, the textile was washed in water and dried repeatedly for 50 cycles, and the weight changes of the textile before and after washing were shown in Fig. S8. The textile has almost no weight loss after washing for 50 times, exhibiting excellent washing durability as well as waterproof ability. In addition, the M-PI-BN/PEG textile still keeps a high thermal conductivity of 4.41 W m^{-1} K^{-1}, only slightly lower than that of PI-BN/PEG textile (5.34 W m^{-1} K^{-1}), indicating its favorable thermoregulating properties after coating PDMS, which could broad its practical application as washable clothing for efficient thermal management.

4. Conclusions

In summary, phase-changeable PI-BN/PEG textile with enhanced thermal conductivity, high phase change enthalpy, advanced flexibility is prepared via freeze-spinning technique in combination with vacuum impregnation. Benefiting from the high thermal conductivity of BN, good mechanical property of PI, combined with high porosity and capillary force of PI-BN aerogel fiber, the resultant phase-changeable PI-BN/PEG textile exhibits high melting enthalpy (125.8 J g^{-1}) and high

thermal conductivity (5.34 W m^{-1} K^{-1}) without leakage during the phase change process. Consequently, the PI-BN/PEG textile has rapid thermal response with longer temperature platform, which could postpone the temperature change upon the change of environment, offering feasible choice for personal cooling/heating in the variable temperature environment. In addition, the phase-changeable PI-BN/PEG textile exhibits excellent cycling stability and retains a high phase change enthalpy after 100 heating-cooling cycles. Moreover, PDMS, as a waterproof layer, was adhered on the surface which endows the phase-changeable textile hydrophobicity, waterproofness and washability, exhibiting great potential for the next generation of intelligent garments.

Credit author statement

Qiaoran Zhang: Investigation, Methodology, Writing - original draft; **Tiantian Xue:** Investigation, Methodology; **Jing Tian:** Software, Validation; **Yi Yang:** Investigation, Methodology; **Wei Fan:** Conceptualization, Supervision, Writing - review & editing; **Tianxi Liu:** Writing - review & editing.

Declaration of competing interest

The authors declare that they have no known competing financial interests or personal relationships that could have appeared to influence the work reported in this paper.

Acknowledgements

This work was supported by the National Natural Science Foundation of China (52073053), Young Elite Scientists Sponsorship Program by CAST (2021QNRC001), Shanghai Rising-Star Program (21QA1400300), Innovation Program of Shanghai Municipal Education Commission (2021-01-07-00-03-E00108), Science and Technology Commission of Shanghai Municipality (20520741100), and China Postdoctoral Science Foundation (2021M690596).

Appendix A. Supplementary data

Supplementary data to this article can be found online at https://doi.org/10.1016/j.compscitech.2022.109541.

References

[1] L.H. Peng, B. Su, A.B. Yu, X.C. Jiang, Review of clothing for thermal management with advanced materials, Cellulose 26 (11) (2019) 6415–6448.
[2] K. Wu, L.P. Yu, C.X. Lei, J.X. Huang, D.Y. Liu, Y. Liu, Y.S. Xie, F. Chen, Q. Fu, Green production of regenerated cellulose/boron nitride nanosheet textiles for static and dynamic personal cooling, ACS Appl. Mater. Interfaces 11 (43) (2019) 40685–40693.
[3] T.T. Gao, Z. Yang, C.J. Chen, Y.J. Li, K. Fu, J.Q. Dai, E.M. Hitz, H. Xie, B.Y. Liu, J. W. Song, B. Yang, L.B. Hu, Three-dimensional printed thermal regulation textiles, ACS Nano 11 (11) (2017) 11513–11520.
[4] Y.B. Guo, K.R. Li, C.Y. Hou, Y.G. Li, Q.H. Zhang, H.Z. Wang, Fluoroalkylsilane-modified textile-based personal energy management device for multifunctional wearable applications, ACS Appl. Mater. Interfaces 8 (7) (2016) 4676–4683.
[5] R. Hu, Y.D. Liu, S.M. Shin, S.Y. Huang, X.C. Ren, W.C. Shu, J.J. Cheng, G.M. Tao, W.L. Xu, R.K. Chen, X.B. Luo, Emerging materials and strategies for personal thermal management, Adv. Energy Mater. 10 (17) (2020) 1903921.
[6] M.E. Darzi, S.I. Golestaneh, M. Kamali, G. Karimi, Thermal and electrical performance analysis of co-electrospun-electrosprayed PCM nanofiber composites in the presence of graphene and carbon fiber powder, Renew. Energy 135 (2019) 719–728.
[7] E.C.B. Noyan, E. Onder, N. Sarier, R. Arat, Development of heat storing poly (acrylonitrile) nanofibers by coaxial electrospinning, Thermochim. Acta 662 (2018) 135–148.
[8] S.Y. Kee, Y. Munusamy, K.S. Ong, H.S. Cornelis Metselaar, S.Y. Chee, K.C. Lai, Thermal performance study of composite phase change material with polyacrylicand conformal coating, Materials 10 (8) (2017) 873–885.
[9] F. Haghighat, S.A. Hosseini Ravandi, M.N. Esfahany, A. Valipouri, Z. Zarezade, Thermal performance of electrospun core-shell phase change fibrous layers at simulated body conditions, Appl. Therm. Eng. 161 (2019) 113924.
[10] P. Sánchez, M.V. Sánchez-Fernandez, A. Romero, J.F. Rodríguez, L. Sánchez-Silva, Development of thermo-regulating textiles using paraffin wax microcapsules, Thermochim. Acta 498 (1–2) (2010) 16–21.
[11] Y. Lu, X.D. Xiao, J. Fu, C.M. Huan, S. Shuai, Y.J. Zhan, Y.Q. Zhu, G. Xu, Novel smart textile with phase change materials encapsulated core-sheath structure fabricated by coaxial electrospinning, Chem. Eng. J. 355 (2019) 532–539.
[12] X. Yu, Y. Li, X. Yin, X.F. Wang, Y.H. Han, Y. Si, J.Y. Yu, B. Ding, Corncoblike, superhydrophobic, and phase-changeable nanofibers for intelligent thermoregulating and water-repellent fabrics, ACS Appl. Mater. Interfaces 11 (42) (2019) 39324–39333.
[13] M. Li, F. Gan, J. Dong, Y. Fang, X. Zhao, Q. Zhang, Facile preparation of continuous and porous polyimide aerogel fibers for multifunctional applications, ACS Appl. Mater. Interfaces 13 (8) (2021) 10416–10427.
[14] H. Yi, L. Xia, S. Song, Three-dimensional montmorillonite/Ag nanowire aerogel supported stearic acid as composite phase change materials for superior solar-thermal energy harvesting and storage, Compos. Sci. Technol. 217 (2022) 109121.
[15] X. Jin, J. Xu, Y. Pan, H. Wang, B. Ma, F. Liu, X. Yan, C. Wu, H. Huang, H. Cheng, C. Hong, X. Zhang, Lightweight and multiscale needle quartz fiber felt reinforced siliconoxycarbide modified phenolic aerogel nanocomposite with enhanced mechanical, insulative and flame-resistant properties, Compos. Sci. Technol. 217 (2022) 109100.
[16] T. Shi, Z. Zheng, H. Liu, D. Wu, X. Wang, Flexible and foldable composite films based on polyimide/phosphorene hybrid aerogel and phase change material for infrared stealth and thermal camouflage, Compos. Sci. Technol. 217 (2022) 109127.
[17] G. Li, G. Hong, D. Dong, W. Song, X. Zhang, Multiresponsive graphene-aerogel-directed phase-change smart fibers, Adv. Mater. 30 (30) (2018), e1801754.
[18] Y. Du, X. Zhang, J. Wang, Z. Liu, K. Zhang, X. Ji, Y. You, X. Zhang, Reaction-spun transparent silica aerogel fibers, ACS Nano 14 (9) (2020) 11919–11928.
[19] Z. Liu, J. Lyu, D. Fang, X. Zhang, Nanofibrous kevlar aerogel threads for thermal insulation in harsh environments, ACS Nano 13 (5) (2019) 5703–5711.
[20] Y. Li, X. Zhang, Electrically conductive, optically responsive, and highly orientated $Ti_3C_2T_x$ MXene aerogel fibers, Adv. Funct. Mater. (2021) 2107767.
[21] Y.J. Wang, Y. Cui, Z.Y. Shao, W.W. Gao, W. Fan, T.X. Liu, H. Bai, Multifunctional polyimide aerogel textile inspired by polar bear hair for ther-moregulation in extreme environments, Chem. Eng. J. 390 (2020) 124623.
[22] X. Li, G. Dong, Z. Liu, X. Zhang, Polyimide aerogel fibers with superior flame resistance, strength, hydrophobicity, and flexibility made via a universal sol-gel confined transition strategy, ACS Nano 15 (3) (2021) 4759–4768.
[23] W. Xia, H. Xiang, Z. Zhou, X. Fei, M. Zhu, Hybridizing rational designed hydrophobic PEG-based derivatives into nanoporous F–SiO_2 as form-stable phase change materials for melt-spun PA6 phase change fibers with a superior washing durability, Compos. Commun. 24 (2021) 100633.
[24] H. Wu, L. Zhao, Y. Si, S. Zhang, J. Yu, B. Ding, Ultralight and superelastic fibrous sponges with effective heat preservation and photo-thermal conversion for personal cold protection, Compos. Commun. 25 (2021) 100766.
[25] C. Xu, E. Li, J. Zeng, Y. Wang, T. Wang, C. Ge, C. Zhang, Q. Wang, T. Gao, Y. Yao, X. Jiang, Y. Zhang, Q. Cheng, X.B. Wang, Interfacial thermal conductance enhancement of BN/PVA composites via plasma activations of fillers, Compos. Commun. 28 (2021) 100963.
[26] K. Fu, Z. Yang, Y. Pei, Y. Wang, B. Xu, Y. Wang, B. Yang, L. Hu, Designing textile architectures for high energy-efficiency human body sweat- and cooling-management, Adv. Fiber Mater. 1 (1) (2019) 61–70.
[27] J. Huang, H. Yu, S.Y.H. Abdalkarim, J. Marek, J. Militky, Y. Li, J. Yao, Electrospun polyethylene glycol/polyvinyl alcohol composite nanofibrous membranes as shape-stabilized solid–solid phase change materials, Adv. Fiber Mater. 2 (3) (2020) 167–177.
[28] S. Pan, H. Peng, Making passive daytime radiative cooling metafabrics on a large scale, Adv. Fiber Mater. 4 (2022) 3–4.
[29] D. Tang, J. Su, M. Kong, Z. Zhao, Q. Yang, Y. Huang, X. Liao, Y. Niu, Preparation and properties of epoxy/BN highly thermal conductive composites reinforced with SiC whisker, Polym. Compos. 37 (9) (2016) 2611–2621.
[30] B.-H. Xie, X. Huang, G.-J. Zhang, High thermal conductive polyvinyl alcohol composites with hexagonal boron nitride microplatelets as fillers, Compos. Sci. Technol. 85 (2013) 98–103.
[31] Q.R. Zhang, Z.W. Li, X.H. Li, L.G. Yu, Z.J. Zhang, Z.S. Wu, Zinc ferrite nanoparticle decorated boron nitride nanosheet: preparation, magnetic field arrangement, and flame retardancy, Chem. Eng. J. 356 (2019) 680–692.
[32] X. Zhao, F. Yang, Z. Wang, P. Ma, W. Dong, H. Hou, W. Fan, T. Liu, Mechanically strong and thermally insulating polyimide aerogels by homogeneity reinforcement of electrospun nanofibers, Compos. B Eng. 182 (2020) 107624.
[33] W. Fan, X. Zhang, Y. Zhang, Y. Zhang, T. Liu, Lightweight, strong, and super-thermal insulating polyimide composite aerogels under high temperature, Compos. Sci. Technol. 173 (2019) 47–52.
[34] T. Nguyen, J.G. Lee, J.S. Park, Fabrication and characterization of coaxial electrospun polyethylene glycol/polyvinylidene fluoride (Core/Sheath) composite non-woven mats, Macromol. Res. 19 (4) (2011) 370–378.
[35] X. Zhang, X. Zhao, T. Xue, F. Yang, W. Fan, T. Liu, Bidirectional anisotropic polyimide/bacterial cellulose aerogels by freeze-drying for super-thermal insulation, Chem. Eng. J. 385 (2020) 123963.
[36] Y. Wu, C.C. Chen, Y.F. Jia, J. Wu, Y. Huang, L.G. Wang, Review on electrospun ultrafine phase change fibers (PCFs) for thermal energy storage, Appl. Energy 210 (2018) 167–181.
[37] P.A. Advincula, A.C. de Leon, B.J. Rodier, J. Kwon, R.C. Advincula, E.B. Pentzer, Accommodating volume change and imparting thermal conductivity by

encapsulation of phase change materials in carbon nanoparticles, J. Mater. Chem. A 6 (6) (2018) 2461–2467.
[38] H. Bi, H. Huang, F. Xu, T. Lin, H. Zhang, F. Huang, Carbon microtube/graphene hybrid structures for thermal management applications, J. Mater. Chem. A 3 (36) (2015) 18706–18710.
[39] W. Liang, G. Zhang, H. Sun, P. Chen, Z. Zhu, A. Li, Graphene–nickel/n-carboxylic acids composites as form-stable phase change materials for thermal energy storage, Sol. Energ. Mat. and Sol. C. 132 (2015) 425–430.
[40] P. Min, J. Liu, X. Li, F. An, P. Liu, Y. Shen, N. Koratkar, Z.Z. Yu, Thermally conductive phase change composites featuring anisotropic graphene aerogels for real-time and fast-charging solar-thermal energy conversion, Adv. Funct. Mater. 28 (51) (2018).
[41] J. Yang, P. Yu, L.S. Tang, R.Y. Bao, Z.Y. Liu, M.B. Yang, W. Yang, Hierarchically interconnected porous scaffolds for phase change materials with improved thermal conductivity and efficient solar-to-electric energy conversion, Nanoscale 9 (45) (2017) 17704–17709.
[42] H. Fang, J. Lin, L. Zhang, A. Chen, F. Wu, L. Geng, X. Peng, Fibrous form-stable phase change materials with high thermal conductivity fabricated by interfacial polyelectrolyte complex spinning, Carbonhyd. Polym. 249 (2020) 116836.
[43] J. Yang, E. Zhang, X. Li, Y. Zhang, J. Qu, Z.Z. Yu, Cellulose/graphene aerogel supported phase change composites with high thermal conductivity and good shape stability for thermal energy storage, Carbon 98 (2016) 50–57.